


## Article

# Processing and Characterization of BCZT-Modified BiFeO<sub>3</sub>-BaTiO<sub>3</sub> Piezoelectric Ceramics

Rizwan Ahmed Malik <sup>1,\*</sup> and Hussein Alrobei <sup>2,\*</sup> 

<sup>1</sup> Department of Metallurgy and Materials Engineering, Faculty of Mechanical and Aeronautical Engineering, University of Engineering and Technology (UET), Taxila 47050, Pakistan

<sup>2</sup> Department of Mechanical Engineering, College of Engineering, Prince Sattam Bin Abdul Aziz University, Al-Kharj 11942, Saudi Arabia

\* Correspondence: rizwanmalik48@yahoo.com (R.A.M.); h.alrobei@psau.edu.sa (H.A.)

**Abstract:** The synthesis of non-lead piezoelectric ceramics  $(1-z)(0.65\text{Bi}_{1.05}\text{Fe}_2\text{O}_3-0.35\text{BaTiO}_3)-z\text{Ba}(\text{Ti}_{0.8}\text{Zr}_{0.2})\text{O}_3-(\text{Ba}_{0.7}\text{Ca}_{0.3})\text{TiO}_3$  using a solid state method and a quenching strategy was investigated. The processing conditions such as the sintering temperature and soaking time were optimized. The patterns of X-ray diffraction (XRD) displayed a pure perovskite structure with no secondary phases. The ferroelectric and piezoelectric characteristics of the samples were considerably improved as a result of the lattice strain. The findings of the experiment revealed that the quenching technique increases the piezoelectric sensor constant of 152 pC/N in optimized conditions. The enhanced piezoelectric sensor constant ( $d_{33}$ ) value at  $z = 0.020$  was ascribed to the incorporation of multi-cationic BCZT, which modified the bond lengths at a unit cell level and gave rise to more flexibility in complex domain switching. This facilitated easier domain alignment in response to the applied field and resulted in an improvement in the electrical properties.

**Keywords:** lead free; piezoelectric; ferroelectric properties; X-ray diffraction



**Citation:** Malik, R.A.; Alrobei, H. Processing and Characterization of BCZT-Modified BiFeO<sub>3</sub>-BaTiO<sub>3</sub> Piezoelectric Ceramics. *Crystals* **2021**, *11*, 1077. <https://doi.org/10.3390/cryst11091077>

Academic Editors: Assem Barakat and Alexander S. Novikov

Received: 11 August 2021  
Accepted: 30 August 2021  
Published: 6 September 2021

**Publisher's Note:** MDPI stays neutral with regard to jurisdictional claims in published maps and institutional affiliations.



**Copyright:** © 2021 by the authors. Licensee MDPI, Basel, Switzerland. This article is an open access article distributed under the terms and conditions of the Creative Commons Attribution (CC BY) license (<https://creativecommons.org/licenses/by/4.0/>).

## 1. Introduction

Lead-based piezoelectric ceramics with superior piezoelectric characteristics are suitable for actuators, energy storage capacitor applications, nanogenerators for energy harvesting, nano-positioners, nanosensors, piezocatalysts, switching and sensing devices, and transducers [1–13]. Lead, on the other hand, has negative impacts on human health [14–16] and causes other environmental issues. Furthermore, these ceramics have a relatively high ferroelectric phase transition temperature ( $T_C$ ) (about 400 °C), making them appropriate for high-temperature operations [17]. Due to environmental concern, lead-based ceramics must therefore be replaced with lead-free piezoelectric materials having high working temperature. A number of experiments have been carried out on lead-free piezoelectric materials. Bismuth ferrite BiFeO<sub>3</sub> (BFO) was discovered to be one of the most versatile and acceptable materials among all lead-free piezoelectric options, owing to its high Curie temperature (830 °C), rhombohedral perovskite structure at ambient temperature, and a high polarization of approximately 100  $\mu\text{C}/\text{cm}^2$  [18,19]. However, the production of impurity phases makes it difficult to achieve a saturated ferroelectric hysteresis loop in pure BFO. Furthermore, the valence changes in Fe ( $\text{Fe}^{3+}$  to  $\text{Fe}^{2+}$ ) and volatilization of  $\text{Bi}^{3+}$  result in a large electrical leakage current [20–23]. As a result of these disadvantages, the practical applicability of BFO has been limited.

Many efforts have been made to make solid solutions using different ABO<sub>3</sub> perovskite ceramics materials in order to mitigate the shortcomings of BiFeO<sub>3</sub>. The electrical characteristics of these solid solutions were improved to some extent. BiFeO<sub>3</sub>-BaTiO<sub>3</sub> (BF-BT) is the most appealing and promising of these solid solutions owing to its high operating temperature [21] and relatively better electrical characteristics. However, the electrical characteristics of BF-BT are affected by excessive BFO leakage current [21]. A quenching

process to address this issue has been reported in several papers [24–27]. Although the piezoelectric properties of BF-BT can be increased by the quenching procedure, they are still not enough in practice; therefore, their piezoelectrical features need to be improved. Recently, Liu et al. [28] reported a large piezoelectric sensor coefficient of  $d_{33} = 600$  pC/N in lead-free  $\text{Ba}(\text{Ti}_{0.8}\text{Zr}_{0.2})\text{O}_3$ - $(\text{Ba}_{0.7}\text{Ca}_{0.3})\text{TiO}_3$  (BCZT) materials. However, the working temperature was found to be below 100 °C.

Based on the literature, the structure and corresponding electrical properties of BF-BT-based systems are vulnerable to processing conditions and modifier elements. In the present work, a new BF-based material was systematically investigated. Lead-free  $(1-z)(0.65\text{Bi}_{1.05}\text{Fe}_2\text{O}_3-0.35\text{BaTiO}_3)$  (BF-BT) was chosen as a base composition and the effect of  $\text{Ba}(\text{Ti}_{0.8}\text{Zr}_{0.2})\text{O}_3$ - $(\text{Ba}_{0.7}\text{Ca}_{0.3})\text{TiO}_3$  (BCZT) content on its properties was studied for the sake of improving the ferroelectric performance. Lead-free BCZT-modified BF-BT solid solutions were prepared by a conventional mixed-oxide method followed by air quenching and the effects of BCZT modification on the structural and electromechanical properties were studied in detail. The processing conditions such as calcination, sintering temperature, and soaking time were optimized, all areas yet to be explored for this piezoceramic system. The effect of BCZT modification on the crystal structure, ferroelectric, and piezoelectric properties were studied. The underlying mechanism of the increased ferroelectric characteristics and their stability, were also examined.

## 2. Experimental Procedure

A solid-state reaction with additional heat treatments was used for the synthesis of piezoelectric ceramics with a composition of  $(1-z)(0.65\text{Bi}_{1.05}\text{Fe}_2\text{O}_3-0.35\text{BaTiO}_3)$  and  $z\text{BCZT}$ , where  $z = 0.00, 0.010, 0.020, \text{ and } 0.030$ . For the raw materials, commercially available carbonates, and metal oxides of  $\text{Bi}_2\text{O}_3$ ,  $\text{Fe}_2\text{O}_3$ ,  $\text{ZrO}_2$ ,  $\text{TiO}_2$ ,  $\text{CaCO}_3$  and  $\text{BaCO}_3$  with a purity greater than 99.9% (Sigma Aldrich Co., St. Louis MO) were used as source materials. The stoichiometric formula was employed to accurately quantify these components, and ethanol with zirconia balls was used for ball-milling for 24 h. Drying and calcining twice at 750 °C for 2 h resulted in phase development in the resultant slurry. Finally, the resultant slurry was ball-milled in ethanol for 4 h with zirconia balls. The calcined powder was pressed at 98 MPa, resulting in 10 mm diameter, disk-shaped ceramic specimens. The pressed discs were sintered at 950 °C, 960 °C, 970 °C, 980 °C, and 990 °C and 1020 °C with a soaking time of 2 h in covered alumina crucibles. Sintering took place at 1020 °C for 2 h, after which the pellets were immediately cooled to ambient temperature.

The crystal structure and phase purity were determined using X-ray diffraction (XRD, X'pert MPD3040, Philips, The Netherlands). Scanning electron microscopy (SEM, JP/JSM5200, Japan) was used to assess morphology. The samples were polarized for 15 min at room temperature in a silicone oil bath with a direct-current (DC) field of 5 kV/mm in order to determine the piezoelectric characteristics. A Berlincourt  $d_{33}$  meter (IACAS, ZJ-6B) was employed to determine the piezoelectric constant. The ferroelectric test system was utilized to detect the hysteresis loops of the polarization against the electric field ( $P$ - $E$ ) in silicon oil at a frequency of 10 Hz and ceramics' loss at different frequencies in the 25–500 °C temperature range.

## 3. Results and Discussion

The X-ray diffraction (XRD) patterns of the synthesized BCZT-modified BF-BT ceramics sintered at various temperatures are shown in Figure 1. It is well understood that the sintering temperature and soaking time are critical for producing high-density ceramics. To achieve optimized sintering conditions, the undoped BF-BT was sintered at different temperatures of 950 °C, 960 °C, 970 °C, 980 °C, and 990 °C with soaking times of 2 h and 4 h. The sintering temperature range was selected based on previous studies of BF-BT-based compositions [24,25]. The increased volatility of Bi at high temperatures destroyed the base composition. No perovskite structure was obtained at a sintering temperature  $T < 1000$  °C. As a result, the optimized sintering temperature for undoped BF-BT ceramics

was determined to be above 1000 °C. Figure 1 shows the effects of sintering temperature on the XRD analysis of undoped BF-BT.

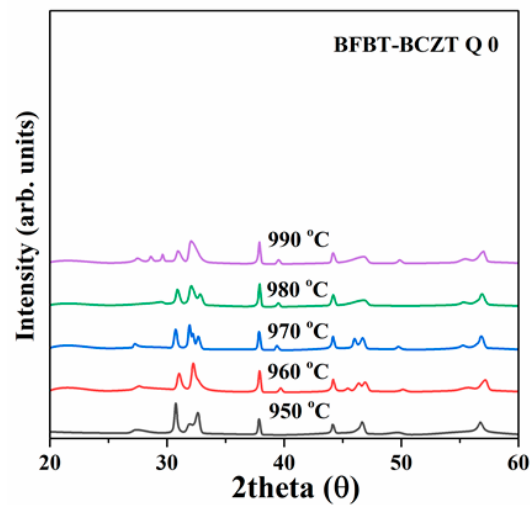


**Figure 1.** X-ray diffraction patterns for BFBT-*z*BCZT (*z* = 0.00) ceramics in the  $2\theta$  ranges of 20–60° sintered at different temperatures.

Figure 2 depicts the XRD results at optimized sintering conditions. All the sintered ceramics show a solid solution that is homogeneous and has a pure perovskite structure with no unwanted secondary phases [29]. The optimized sintering temperature for undoped BF-BT ceramics was determined to be 1020 °C with a 2 h soaking period. At these conditions, a single pseudo-cubic structure was obtained, showing that the synthesized materials had a perovskite crystal structure [29,30]. This demonstrates that the thermal treatment was quite efficient in achieving a stable phase structure by suppressing undesirable phases.

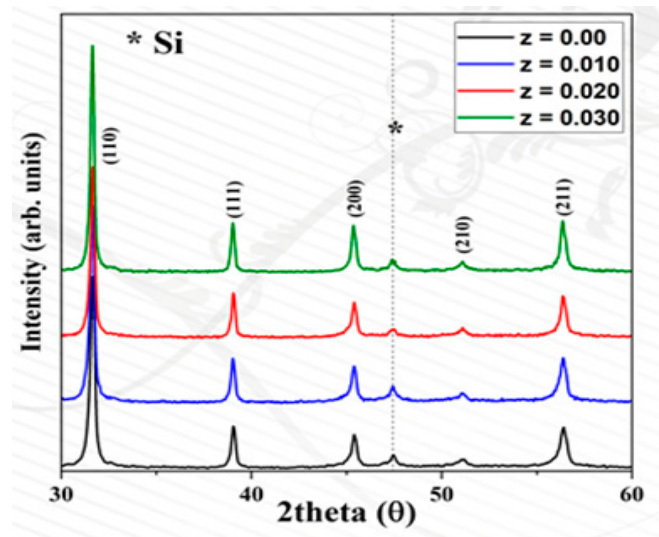


**Figure 2.** X-ray diffraction patterns for BFBT-*z*BCZT (*z* = 0.00–0.030) ceramics in the  $2\theta$  ranges of 30–60° sintered at optimized conditions.

Generally, the microstructure of the ceramics determines their electrical properties. Therefore, SEM micrographs were analyzed, as shown in Figure 3, to investigate the microstructure of the BCZT-modified BF-BT sintered ceramics. All ceramics were well-sintered with a close-packed structure with clear grains and grain boundaries. This shows that no melting occurred at these sintering conditions. For the sample *z* = 0.00, an inhomogeneous microstructure was observed with a mixture of small-sized and large-sized

grains. However, densification improved in samples  $z = 0.010$  and  $0.020$ . Here, as can be seen from Figure 3, the sample  $z = 0.020$  showed better densification with void free and relatively homogeneous micrographs as compared to the other sintered samples. A reduction in porosity is an important factor for enhancing ferroelectric or piezoelectric characteristics [31]. The sample  $z = 0.030$  showed an inhomogeneous microstructure with small voids that suggests a decrease in densification in this sample. Overall, grain size decreased from  $6.6 \mu\text{m}$  for sample  $z = 0.00$  to  $5.8 \mu\text{m}$  for sample  $z = 0.030$ .

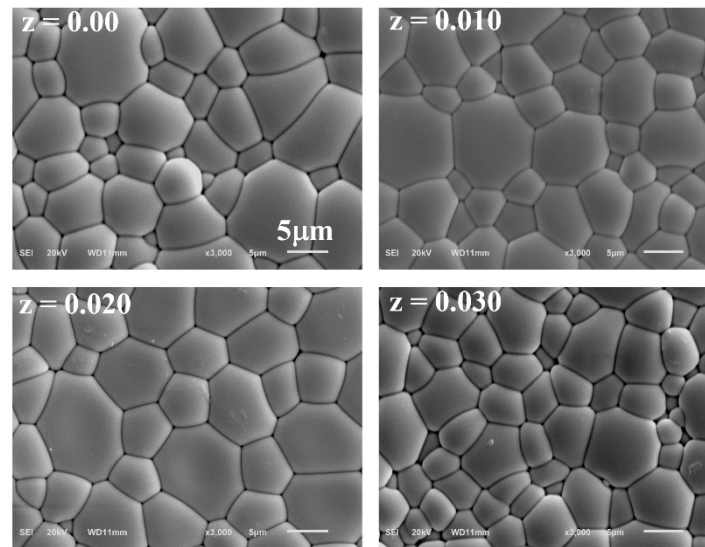


**Figure 3.** SEM micrographs of BFBT-zBCZT ( $z = 0.00$ – $0.030$ ) samples.

The density of the ceramics is shown in Figure 4 at a sintering temperature of  $1020 \text{ }^\circ\text{C}$  and a soaking time of 2 h. The unmodified ceramic sample had a density of  $6.72 \text{ g/cm}^3$ , while the 2-mol.% modified sample showed an increased density value of  $7.25 \text{ g/cm}^3$  (~96% densification), which began to drop at high dopant concentrations.

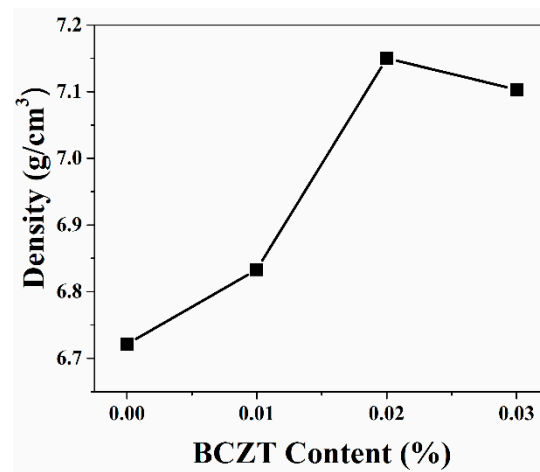


**Figure 4.** Density measurement of BFBT-zBCZT ( $z = 0.00$ – $0.030$ ) samples.

Figure 5 shows the polarization-electric field ( $P$ - $E$ ) hysteresis loops of BT-BF ceramics sintered at various temperatures with a soaking time of 2 h at an applied field of 2.5, 3 and  $4 \text{ kV/cm}$ , which are indicated by blue, black, and red, respectively. Up to a sintering temperature of  $1010 \text{ }^\circ\text{C}$ , the absence of the ferroelectric  $P$ - $E$  loop of sintered samples demonstrated the paraelectric phase of the material. As the sintering temperature increased ( $1020 \text{ }^\circ\text{C}$ ), the ferroelectric property of the material was progressively improved [29,30].

Hence, the optimal sintering conditions were found to be 1020 °C and a soaking time of 2 h for these ceramics.

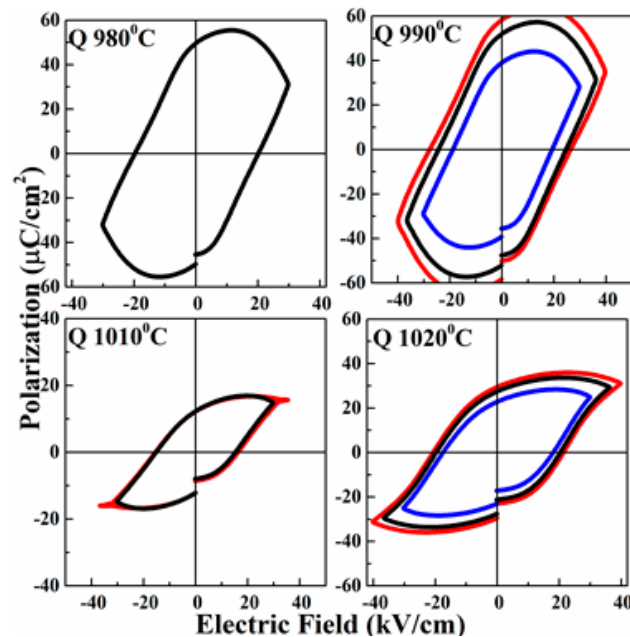


**Figure 5.** Ferroelectric properties of BFBT–zBCZT ( $z = 0.00$ ) sample sintered at 980 °C, 990 °C, 1010 °C and 1020 °C.

Well-saturated  $P$ – $E$  hysteresis loops were observed with no pinching for all compositions sintered at optimized conditions, which confirmed normal ferroelectric behaviour [21–27]. BCZT incorporation successfully enhanced the ferroelectric characteristics of the base composition ( $z = 0.00$ ), as indicated by an increase in remnant polarization  $P_r$  and a decrease in coercive field  $E_c$ , as illustrated in Figure 6. The  $P_r$  and  $E_c$  values change from  $\sim 25 \mu\text{C}/\text{cm}^2$  and  $\sim 28 \text{ kV}/\text{cm}$  for pure ceramics to  $\sim 28 \mu\text{C}/\text{cm}^2$  and  $\sim 26 \text{ kV}/\text{cm}$  for  $z = 0.020$ , respectively. These results are comparable to previous reports on BF-based systems [10–13]. Both  $P_r$  and  $E_c$  dropped as the BCZT content increased. This can be linked to inhomogeneous grain size, a drop in density and the presence of porosity in the  $z = 0.030$  sample. Also, it can be seen that very small grains were developed between larger grains. It is proposed that inhomogeneous grain size, the reduction in density, the presence of porosity and very small grains between larger grains resulted in the slanted  $P$ – $E$  loop for this sample.

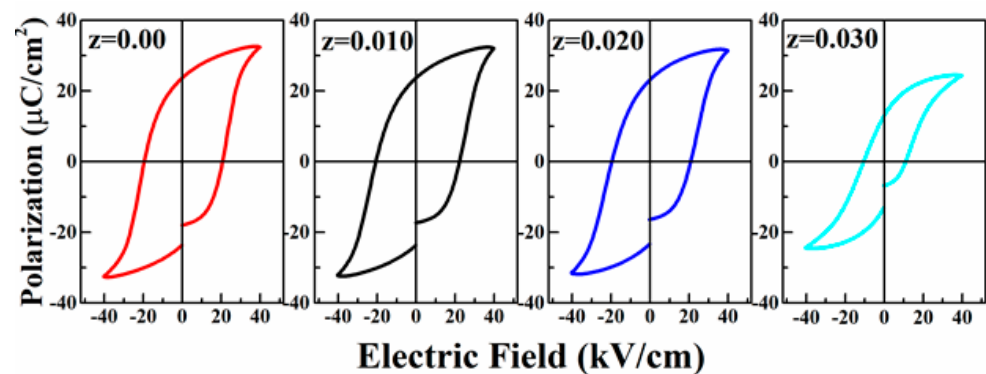


**Figure 6.** Ferroelectric properties of BFBT–zBCZT ( $z = 0.00$ – $0.030$ ) samples at optimized conditions.

Internal stresses are generated at the grain boundaries during poling. Domain re-orientation affects the re-orientation of spontaneous strain, which can modify the dimensions of specific grains. Intergranular stresses are higher in ceramics with very small

grains present between larger grains due to higher grain boundary density. Due to higher intergranular stresses at these grain boundaries, back fields are exerted that inhibit domain reversal and lower saturation polarization. When the field is removed, the high intergranular stresses force the domains to switch back and lower the Pr. The polarization results are in good agreement with the microstructural results [32].

In contrast to BNT-based systems, all samples in the examined compositional range demonstrated conventional ferroelectric-like behaviour without visible pinching and the corresponding non-ergodic to ergodic transition [22–27]. This behaviour may be linked to the differences in domain morphologies and role of defects in the BF and BNT-based systems. Recently, in situ poling synchrotron X-ray diffraction revealed that the pseudo-cubic symmetry preserved during and after the application of electric fields and piezoelectric properties were linked to the presence of multi-symmetry polar nanoregions, which allowed for a high average distortion in the applied field direction [33]. In another study, by using in situ poling synchrotron XRD, the absence of long-range ferroelectric order and the retention of short-range polar order was proposed in BF-based ceramics [34]. However, the exact mechanism in BF-based systems is still unclear and needs further sophisticated studies.

All poled samples were aged for 24 h before the measurement of the piezoelectric sensor coefficient ( $d_{33}$ ). For each sample, three readings were taken, and the mean was calculated. The piezoelectric sensor coefficient was enhanced from  $\sim 50$  pC/N for an unmodified sample to  $\sim 152$  pC/N for a 2 mol.% modified sample, as shown in Figure 7, which is in good agreement with the ferroelectric properties. This value is better than the previously reported values for lead-free piezoelectric ceramics, as shown in Table 1 [35–43].

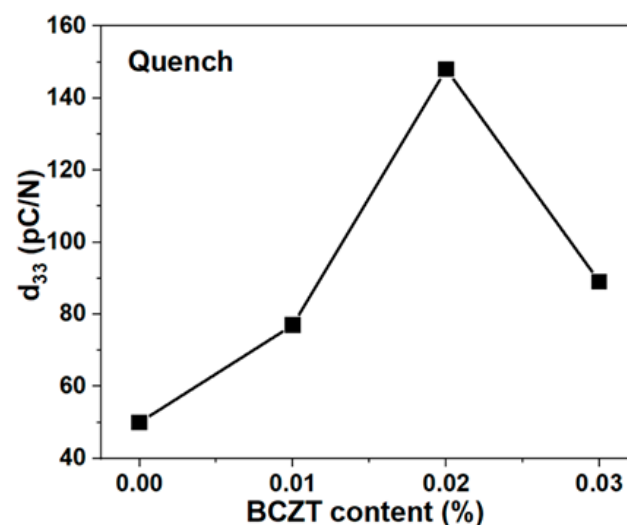


**Figure 7.** Variation in room temperature piezoelectric constant ( $d_{33}$ ) of BFBT-zBCZT ( $z = 0.00$ – $0.030$ ) ceramics.

This increase in  $d_{33}$  at  $z = 0.020$  may be ascribed to the incorporation of multi-cationic BZCT, which modified the bond lengths at a unit cell level and gave rise to more flexibility in the complex domain switching. Consequently, the enhancement in the  $d_{33}$  value was observed for very flexible (at a unit cell level) compositions. Despite the fact that no discernible structural change was observed within the XRD detection limit for all specimens, the electrical properties show that the addition of BCZT to the base BF-BT lattice has a significant effect. The observed broadening of the peaks, in contrast to a pure cubic structure, may indicate the presence of some non-cubic distortion or pseudo-cubic phase that is required for ferroelectricity to exist in materials. The variation in the electromechanical properties strongly suggests that the origin of the high piezoelectric property is linked to the crystal structure morphotropic phase boundary.

**Table 1.** Comparison of the piezoelectric constant of various BF-BT ceramics.

| Materials   | $d_{33}$<br>(pC/N) | Year | References   |
|---|--------------------|------|--------------|
| BiFeO <sub>3</sub> –BaTiO <sub>3</sub> –Bi <sub>0.5</sub> K <sub>0.5</sub> TiO <sub>3</sub>     | 135                | 2013 | [35]         |
| 0.65BFGa–0.35BT   | 145                | 2018 | [36]         |
| 0.675BF–0.325BT–xLT   | 145                | 2018 | [37]         |
| 0.75B <sub>0.975</sub> Nd <sub>0.025</sub> F <sub>–0.25</sub> BT+Mn                             | 140                | 2018 | [38]         |
| 0.73BF–0.25BT–0.02LCM + Mn  | 108                | 2015 | [39]         |
| 0.99(0.67BF–0.33BT)–0.01LN  | 146                | 2017 | [40]         |
| 0.60BF–0.40BT–0.02BZT   | 50                 | 2017 | [41]         |
| 0.75BF–0.25BT   | 47                 | 2009 | [42]         |
| 0.65Bi <sub>1.05</sub> Fe <sub>1–x</sub> Ga <sub>x</sub> O <sub>3</sub> –0.35BaTiO <sub>3</sub> | 140                | 2019 | [43]         |
| BF–BT–BCZT  | 152                | 2021 | Current Work |

#### 4. Conclusions

In this work, an air quenching approach and a solid-state reaction method were used to study the synthesis of lead-free BCZT-modified BF-BT piezoelectric ceramics. X-ray diffraction patterns revealed a pure perovskite structure without any secondary phases. An enhanced piezoelectric sensor constant of 152 pC/N was observed with improved remnant polarization  $P_r \sim 28 \mu\text{C}/\text{cm}^2$ . The combination of grain size effect, densification, and hence improved polarization  $P_r$  is thought to be responsible for the enhanced piezoelectric properties in the optimized composition. This study suggests that the ferroelectric properties of the BF-BT system were significantly improved by BCZT incorporation.

**Author Contributions:** Conceptualization, methodology, formal analysis, investigation, and writing—original draft preparation, R.A.M.; writing—review and editing, R.A.M. and H.A.; supervision, R.A.M. and H.A.; project administration, R.A.M. and H.A. All authors have read and agreed to the published version of the manuscript.

**Funding:** This project was supported by the Deanship of Scientific Research at Prince Sattam bin Abdulaziz University, under the research project no. 2020/01/17063.

**Conflicts of Interest:** The authors declare no conflict of interest.

#### References

- Hao, J.; Li, W.; Zhai, J.; Chen, H. Progress in high-strain perovskite piezoelectric ceramics. *Mater. Sci. Eng. R Rep.* **2019**, *135*, 1–57. [CrossRef]
- Zheng, T.; Wu, J.; Xiao, D.; Zhu, J. Recent development in lead-free perovskite piezoelectric bulk materials. *Prog. Mater. Sci.* **2018**, *98*, 552–624. [CrossRef]
- Malik, R.A.; Hussain, A.; Zaman, A.; Maqbool, A.; Rahman, J.U.; Song, T.K.; Kim, W.J.; Kim, M.H. Structure–property relationship in lead-free A- and B-site co-doped Bi<sub>0.5</sub>(Na<sub>0.84</sub>K<sub>0.16</sub>)<sub>0.5</sub>TiO<sub>3</sub>–SrTiO<sub>3</sub> incipient piezoceramics. *RSC Adv.* **2015**, *5*, 96953–96964. [CrossRef]
- Rödel, J.; Webber, K.G.; Dittmer, R.; Jo, W.; Kimura, M.; Damjanovic, D. Transferring lead-free piezoelectric ceramics into application. *J. Eur. Ceram. Soc.* **2015**, *35*, 1659–1681. [CrossRef]
- Zeeshan; Panigrahi, B.K.; Ahmed, R.; Mehmood, M.U.; Park, J.C.; Kim, Y.; Chun, W. Operation of a low-temperature differential heat engine for power generation via hybrid nanogenerators. *Appl. Energy* **2021**, *285*, 116385. [CrossRef]
- Hajra, S.; Tripathy, A.; Panigrahi, B.K.; Choudhary, R.N.P. Development and excitation performance of lead-free electronic material: Eu and Fe doped Bi<sub>0.5</sub>Na<sub>0.5</sub>TiO<sub>3</sub> for filter application. *Mater. Res. Express* **2019**, *6*, 076304. [CrossRef]
- Hajra, S.; Sahoo, S.; Mishra, T.; De, M.; Rout, P.K.; Choudhary, R.N.P. Studies of structural, dielectric and electrical characteristics of BaTiO<sub>3</sub>–BiFeO<sub>3</sub>–CaSnO<sub>3</sub> electronic system. *J. Mater. Sci. Mater. Electron.* **2018**, *29*, 7876–7884. [CrossRef]
- Briscoe, J.; Dunn, S. Piezoelectric nanogenerators—A review of nano structured piezoelectric energy harvesters. *Nano Energy* **2015**, *14*, 15–29. [CrossRef]
- Hanani, Z.; Izzanar, I.; Amjoud, M.; Mezzane, D.; Lahcini, M.; Ursic, H.; Prah, U.; Saadoune, I.; Marssi, M.E.; Lukyanchuk, I.A.; et al. Lead-free nanocomposite piezoelectric nanogenerator film for biomechanical energy harvesting. *Nano Energy* **2021**, *81*, 105661. [CrossRef]
- Mistewicz, K. Recent advances in ferroelectric nanosensors: Toward sensitive detection of gas, mechano-thermal signals, and radiation. *J. Nanomater.* **2018**, *2018*, 2651056. [CrossRef]

11. Lee, H.S.; Chung, J.; Hwang, G.T.; Jeong, C.K.; Jung, Y.; Kwak, J.H.; Kang, H.; Byun, M.; Kim, W.D.; Hur, S.; et al. Flexible inorganic piezoelectric acoustic nanosensors for biomimetic artificial hair cells. *Adv. Funct. Mater.* **2014**, *24*, 6914–6921. [CrossRef]
12. Qian, W.; Yang, W.; Zhang, Y.; Bowen, C.R.; Yang, Y. Piezoelectric materials for controlling electro-chemical processes. *Nano-Micro Lett.* **2020**, *12*, 149. [CrossRef]
13. Mistewicz, K.; Kepinska, M.; Nowak, M.; Sasiela, A.; Zubko, M.; Stróz, D. Fast and efficient piezo/photocatalytic removal of methyl orange using SbSI nanowires. *Materials* **2020**, *13*, 4803. [CrossRef]
14. Adnan, M.; Hussain, A.; Rahman, J.U.; Malik, R.A.; Song, T.K.; Kim, M.-H.; Kim, W.-J. Composition-dependent structural, dielectric and ferroelectric responses of lead-free  $\text{Bi}_{0.5}\text{Na}_{0.5}\text{TiO}_3\text{-SrZrO}_3$  ceramics. *J. Korean Phys. Soc.* **2016**, *68*, 1430–1438.
15. Rahman, J.U.; Hussain, A.; Adnan, M.; Malik, R.A.; Song, T.K.; Kim, M.-H.; Lee, S.; Kim, W.-J. Effect of donor doping on the ferroelectric and the piezoelectric properties of lead-free  $0.97(\text{Bi}_{0.5}\text{Na}_{0.5}\text{Ti}_{1-x}\text{Nb}_x)\text{O}_3\text{-}0.03\text{BaZrO}_3$  ceramics. *J. Korean Phys. Soc.* **2015**, *67*, 1240–1245. [CrossRef]
16. Rahman, J.U.; Hussain, A.; Adnan, M.; Malik, R.A.; Kim, M.S.; Kim, M.-H. Effect of sintering temperature on the electromechanical properties of  $0.945\text{Bi}_{0.5}\text{Na}_{0.5}\text{TiO}_3\text{-}0.055\text{BaZrO}_3$  ceramics. *J. Korean Phys. Soc.* **2015**, *66*, 1072–1076. [CrossRef]
17. Cheon, C.I.; Choi, J.H.; Kim, J.S.; Zang, J.; Fromling, T.; Rodel, J.; Jo, W. Role of  $(\text{Bi}_{1/2}\text{K}_{1/2})\text{TiO}_3$  in the dielectric relaxations of  $\text{BiFeO}_3\text{-}(\text{Bi}_{1/2}\text{K}_{1/2})\text{TiO}_3$  ceramics. *J. Appl. Phys.* **2016**, *119*, 15410. [CrossRef]
18. Ryu, G.H.; Hussain, A.; Lee, M.H.; Malik, R.A.; Song, T.K.; Kim, W.J.; Kim, M.H. Lead-free high performance Bi ( $\text{Zn}_{0.5}\text{Ti}_{0.5}$ )  $\text{O}_3\text{-modified BiFeO}_3\text{-BaTiO}_3$  piezoceramics. *J. Eur. Ceram. Soc.* **2018**, *38*, 4414–4421. [CrossRef]
19. Lee, M.H.; Kim, D.J.; Park, J.S.; Kim, S.W.; Song, T.K.; Kim, M.H.; Kim, W.J.; Do, D.; Jeong, I.K. High-performance lead-free piezoceramics with high curie temperatures. *Adv. Mater.* **2015**, *27*, 6976–6982. [CrossRef] [PubMed]
20. Rojac, T.; Bencan, A.; Malic, B.; Tutuncu, G.; Jones, J.L.; Daniels, J.E.; Damjanovic, D.  $\text{BiFeO}_3$  ceramics: Processing, electrical, and electromechanical properties. *J. Am. Ceram. Soc.* **2014**, *97*, 1993–2011. [CrossRef]
21. Khan, S.A.; Ahmed, T.; Akram, F.; Bae, J.; Choi, S.Y.; Thanh, T.T.; Kim, M.; Song, T.K.; Sung, Y.S.; Kim, M.H.; et al. Effect of sintering temperature on the electrical properties of pristine BF-35BT piezoelectric ceramics. *J. Korean Ceram. Soc.* **2020**, *57*, 290–295. [CrossRef]
22. Lee, M.H.; Kim, D.J.; Choi, H.I.; Kim, M.-H.; Song, T.K.; Kim, W.-J.; Park, J.S.; Do, D. Low sintering temperature for lead-free  $\text{BiFeO}_3\text{-BaTiO}_3$  ceramics with high piezoelectric performance. *J. Am. Ceram. Soc.* **2019**, *102*, 2666–2674.
23. Lee, M.H.; Kim, D.J.; Choi, H.I.; Kim, M.-H.; Song, T.K.; Kim, W.-J.; Do, D. Thermal quenching effects on the ferroelectric and piezoelectric properties of  $\text{BiFeO}_3\text{-BaTiO}_3$  ceramics. *ACS Appl. Electron. Mater.* **2019**, *1*, 1772–1780. [CrossRef]
24. Akram, F.; Malik, R.A.; Khan, S.A.; Hussain, A.; Lee, S.; Lee, M.-H.; In, C.H.; Song, T.-K.; Kim, W.-J.; Sung, Y.S.; et al. Electromechanical properties of ternary  $\text{BiFeO}_3\text{-}0.35\text{BaTiO}_3\text{-BiGaO}_3$  piezoelectric ceramics. *J. Electroceram.* **2018**, *41*, 93–98. [CrossRef]
25. Akram, F.; Hussain, A.; Malik, R.A.; Song, T.-K.; Kim, W.-J.; Kim, M.-H. Synthesis and electromechanical properties of  $\text{LiTaO}_3\text{-modified BiFeO}_3\text{-BaTiO}_3$  piezoceramics. *Ceram. Int.* **2017**, *43*, S209–S213. [CrossRef]
26. Habib, M.; Lee, M.H.; Akram, F.; Kim, M.-H.; Kim, W.-J.; Song, T.K. Temperature-insensitive piezoelectric properties of lead-free  $\text{BiFeO}_3\text{-BaTiO}_3$  ceramics with high Curie temperature. *J. Alloys Compd.* **2021**, *851*, 156788. [CrossRef]
27. Habib, M.; Lee, M.H.; Choi, H.I.; Kim, M.-H.; Kim, W.-J.; Song, T.K. Phase evolution and origin of the high piezoelectric properties in lead-free  $\text{BiFeO}_3\text{-BaTiO}_3$  ceramics. *Ceram. Int.* **2020**, *46*, 22239–22252. [CrossRef]
28. Liu, W.; Ren, X. Large piezoelectric effect in Pb-free ceramics. *Phys. Rev. Lett.* **2009**, *103*, 257602. [CrossRef]
29. Alzaid, M.; Alsah, F.; Malik, R.A.; Maqbool, A.; Almoisheer, N.; Hadia, N.M.A.; Mohamed, W.S.  $\text{LiTaO}_3$  assisted giant strain and thermally stable energy storage response for renewable energy storage applications. *Ceram. Int.* **2021**, *47*, 15710–15721. [CrossRef]
30. Malik, R.A.; Zaman, A.; Hussain, A.; Maqbool, A.; Song, T.K.; Kim, W.-J.; Sung, Y.S.; Kim, M.-H. Temperature invariant high dielectric properties over the range  $200\text{ }^\circ\text{C}\text{-}500\text{ }^\circ\text{C}$  in  $\text{BiFeO}_3$  based ceramics. *J. Eur. Ceram. Soc.* **2018**, *38*, 2259–2263. [CrossRef]
31. Fernandez-Benavides, D.A.; Gutierrez-Perez, A.I.; Benitez-Castro, A.M.; Ayala-Ayala, M.T.; Moreno-Murguia, B.; Muñoz-Saldaña, J. Comparative study of ferroelectric and piezoelectric properties of BNT-BKT-BT ceramics near the phase transition zone. *Materials* **2018**, *11*, 361. [CrossRef] [PubMed]
32. McKinnon, R.A. Grain Size Effect in Lead-Free  $\text{Bi}_{0.5}\text{Na}_{0.5}\text{TiO}_3\text{-Based Materials: Exploring the Ferroelectric Behaviour}$ . 2015. Available online: <https://qmro.qmul.ac.uk/xmlui/handle/123456789/12899> (accessed on 24 August 2021).
33. Wang, G.; Fan, Z.; Murakami, S.; Lu, Z.; Hall, D.A.; Sinclair, D.C.; Feteira, A.; Tan, X.; Jones, J.L.; Kleppe, A.K.; et al. Origin of the large electrostrain in  $\text{BiFeO}_3\text{-BaTiO}_3$  based lead-free ceramics. *J. Mater. Chem. A* **2019**, *7*, 21254–21263. [CrossRef]
34. Lu, Z.; Wang, G.; Li, L.; Huang, Y.; Feteira, A.; Bao, W.; Kleppe, A.K.; Xu, F.; Wang, D.; Reaney, I.M. In situ poling X-ray diffraction studies of lead-free  $\text{BiFeO}_3\text{-SrTiO}_3$  ceramics. *Mater. Today Phys.* **2021**, *19*, 100426. [CrossRef]
35. Lin, D.; Zheng, Q.; Li, Y.; Wan, Y.; Li, Q.; Zhou, W. Microstructure, ferroelectric, and piezoelectric properties of  $\text{Bi}_{0.5}\text{K}_{0.5}\text{TiO}_3\text{-modified BiFeO}_3\text{-BaTiO}_3$  lead-free ceramics with high Curie temperature. *J. Eur. Ceram. Soc.* **2013**, *33*, 3023–3036. [CrossRef]
36. Khan, S.A.; Malik, R.A.; Akram, F.; Hussain, A.; Song, T.-K.; Kim, W.-J.; Kim, M.-H. Synthesis, and electrical properties of  $0.65\text{Bi}_{1.05}\text{Fe}_{1-x}\text{Ga}_x\text{O}_3\text{-}0.35\text{BaTiO}_3$  piezoceramics by air quenching process. *J. Electroceram.* **2018**, *41*, 60–66. [CrossRef]
37. Akram, F.; Malik, R.A.; Lee, S.; Pasha, R.A.; Kim, M.H. Enhanced piezoelectric properties of  $(1-x)[0.675\text{BiFeO}_3\text{-}0.325\text{BaTiO}_3]\text{-xLiTaO}_3$  ternary system by air quenching. *Korean J. Mater. Res.* **2018**, *28*, 489–494. [CrossRef]
38. Wang, D.; Fan, Z.; Zhou, D.; Khesro, A.; Murakami, S.; Feteira, A.; Zhao, Q.; Tan, X.; Reaney, I.M. Bismuth ferrite-based leadfree ceramics and multilayers with high recoverable energy density. *J. Mater. Chem. A* **2018**, *6*, 4133. [CrossRef]



39. Luo, L.; Jiang, N.; Zou, X.; Shi, D.; Sun, T.; Zheng, Q.; Xu, C.; Lam, K.H.; Lin, D. Phase transition, piezoelectric, and multiferroic properties of La (Co<sub>0.5</sub>Mn<sub>0.5</sub>) O<sub>3</sub>-modified BiFeO<sub>3</sub>-BaTiO<sub>3</sub> lead-free ceramics. *Phys. Status Solidi A* **2015**, *212*, 2012–2022. [[CrossRef](#)]
40. Malik, R.A.; Hussain, A.; Song, T.K.; Kim, W.J.; Ahmed, R.; Sung, Y.S.; Kim, M.H. Enhanced electromechanical properties of (1-x) BiFeO<sub>3</sub>-BaTiO<sub>3</sub>-xLiNbO<sub>3</sub> ceramics by quenching process. *Ceram. Int.* **2017**, *43*, S198–S203. [[CrossRef](#)]
41. Liu, Z.; Zheng, T.; Zhao, C.; Wu, J. Composition design and electrical properties in BiFeO<sub>3</sub>-BaTiO<sub>3</sub>-Bi (Zn<sub>0.5</sub>Ti<sub>0.5</sub>) O<sub>3</sub> leadfree ceramics. *J. Mater. Sci. Mater. Electron.* **2017**, *28*, 13076. [[CrossRef](#)]
42. Leontsev, S.O.; Eitel, R.E. Dielectric and piezoelectric properties in Mn-modified (1 - x) BiFeO<sub>3</sub>-xBaTiO<sub>3</sub> ceramics. *J. Am. Ceram. Soc.* **2009**, *92*, 2957. [[CrossRef](#)]
43. Khan, S.A.; Akram, F.; Malik, R.A.; Hussain, A.; Kim, J.C.; Song, T.K.; Kim, W.-J.; Sung, Y.S.; Kim, M.-H.; Lee, S. Effects of cooling rate on the electrical properties of Pb-free BF-BT ceramics. *Ferroelectrics* **2019**, *553*, 76–82. [[CrossRef](#)]